Available online at www.sciencedirect.com
SCIENCE DIRECT
ELSEVIER
Polymer 46 (2005) 5268–5277
polymer
www.elsevier.com/locate/polymer

Toward an understanding of thermoresponsive transition behavior of hydrophobically modified *N*-isopropylacrylamide copolymer solution

Zhiqiang Cao[a], Wenguang Liu[a,*], Peng Gao[a], Kangde Yao[a], Hexian Li[b], Guochang Wang[b]

[a]*Research Institute of Polymeric Materials, Tianjin University, Tianjin 300072, People's Republic of China*
[b]*State Key Laboratory of Functional Polymer Materials for Adsorption and Separation, Nankai University, Tianjin 300071, People's Republic of China*

Received 5 January 2005; received in revised form 14 April 2005; accepted 21 April 2005

Abstract

Poly(*N*-isopropylacrylamide-*co*-vinyl laurate)(PNIPAAm-*co*-VL) copolymers were prepared at various feed ratios via conventional radical random copolymerization. The formation, composition ratios and molecular weight of copolymers were examined. The thermoresponsive behaviors of PNIPAAm and PNIPAAm-*co*-VL solutions at low and high concentrations were intensively investigated by turbidity measurement, Micro-DSC, temperature-variable state fluorescence, ^{1}H NMR and dynamic light scattering (DLS). Several important results were obtained that (1) incorporation of PVL results in much lower and broader LCST regions of the copolymer solutions, and facilitates the formation of hydrophobic microdomains far below LCST, causing a pronounced aggregation in solutions (2) temperature-variable ^{1}H NMR spectra shows that during the phase transition, the 'penetration' of PNIPAAm into the hydrophobic core is a process accompanied with a transition of isopropyl from hydration to dehydration as well as a self-aggregation of hydrophobic chains at different temperature stages (3) according to the ^{1}H NMR spectra of polymer solutions obtained at varied temperatures, the microdomains from hydrophobic VL moieties have a different accessibility for isopropyl groups and the entire chains during phase transition (4) temperature-variable DLS demonstrates that the temperature-induced transition behavior of copolymers is supposedly divided into three stages: pre-LCST aggregation (<20 °C), coil–globule transition at LCST (20–25 °C) and post-LCST aggregation (>25 °C).

Keywords: Poly(*N*-isopropylacrylamide); Vinyl laurate; Thermoresponsive

1. Introduction

Among the stimuli-sensitive polymers, poly(*N*-isopropylacrylamide), abbreviated as PNIPAAm, has attracted probably the most attention due to its sharp transition behavior and well-defined lower critical solution temperature (LCST) in aqueous medium around 32–34 °C which is close to the body temperature [1–3]. Polymer chains undergo a reversible dehydration and hydration upon heating and cooling, causing a coil-to-globule transition [4]. This characteristic has been exploited for the application in temperature sensitive nonviral vector for gene delivery [5], smart culture surface for controllable cell adhesion and detachment [6], switchable surface between superhydrophilicity and superhydrophobicity [7], temperature-tunable catalyst [8] and in situ-formable scaffold [9,10].

Relatively recently, hydrophobically modified poly(*N*-isopropylacrylamides) (HM-PNIPAAms) such as NIPAAm and *n*-alkylacrylamides random copolymers have been prepared and studied [11,12]. In these HM-PNIPAAms, the hydrophobic chains associated in dilute solution leading to micellization with core-corona structure consisting of hydrophobic core and hydrated PNIPAAm corona layer. And LCSTs still existed, but were greatly lowered by hydrophobic moieties, which was supposed to make LCST phenomenon more understandable by intensifying hydrophobic effects and thus making possible the differentiation of the effect of hydrogen bonding and hydrophobicity on the aggregation and phase separation process. More recently, pH/temperature sensitive copolymers of *N*-isopropylacrylamide and *n*-glycine acrylamide were prepared, and it was evidenced by fluorescence spectroscopy, dynamic light scattering and microcalorimetry that varying pH or

* Corresponding author.
E-mail address: wgliu@tju.edu.cn (W. Liu).

0032-3861/$ - see front matter © 2005 Elsevier Ltd. All rights reserved.
doi:10.1016/j.polymer.2005.04.050

temperature induced a transition from coil to globule of copolymer backbone in solution, but the hydrophobic core of micelles was not affected [13,14]. The RAFT polymerization-derived amphiphilic diblock copolymers of *N*-isopropylacrylamide with either styrene or *tert*-butyl methacrylate were shown to form micelles or large aggregates depending on the lengths of the blocks when copolymers were transferred from an organic solvent to water; heating resulted in the collapse of large aggregates, which occurred slowly over a broad temperature range [15]. A thermoreversible PNIPAAm-lipid conjugate was reported to self-assemble at room temperature to form liquid crystalline gels with an expanded lamellar structure, and transform into a collapsed lamellar structure with a modest increase in temperature [16]. Benee et al reported that poly(*N*-isopropylacrylamide-*co*-vinyl laurate) microgel dispersions could form irreversible aggregates or macrogels when heated in a salt solution above a critical electrolyte concentration [17].

To our best knowledge, to date, a comprehensive investigation into temperature dependent phase transition of the random HM-PNIPAAm aqueous system is still in scarcity in literature. To get a deeper understanding toward the thermoresponsive behavior of HM-PNIPAAm solution, in this work, poly(*N*-isopropylacrylamide-*co*-vinyl laurate) (PNIPAAm-*co*-VL) copolymers were synthesized with conventional radical random copolymerization technique. We will focus on elucidation of the formation of hydrophobic microdomains, and the variation in hydrated state of isopropyl groups during the 'penetration' of the whole PNIPAAm chains into hydrophobic cores. The discrepancy in the contribution of isopropyl groups and entire polymer chains during transition will be examined. The stage of transition for PNIPAAm-*co*-VL solution will also be proposed.

2. Experimental part

2.1. Materials

N-Isopropylacrylamide (NIPAAm, Aldrich Chemical Co.) was purified by recrystallization in hexane and dried in vacuo at 25 °C. Vinyl laurate (VL, Fluka Co.) was used as received. 2,2-Azoisobutyronitrile (AIBN, Fluka) was twice recrystallized from methanol and dried in vacuo. Tetrahydrofuran (THF) and ethyl ether were used after distillation.

2.2. Synthesis of PNIPAAm-co-PVL copolymers, PNIPAAm and PVL homopolymers

PNIPAAm-*co*-PVL was synthesized by free radical polymerization using AIBN as an initiator in THF. Take molar feed ratio of NIPAAm to VL, 2/1 for example, 4.95 g of NIPAAm, 4.946 g of VL and 35 ml THF were mixed in a four-mouth flask equipped with a condenser and liquid-sealed tube. After 30 min nitrogen flow to remove oxygen, 0.1225 g of AIBN in 1 ml THF was added and the reaction mixture was stirred in an oil bath at 60 °C for 8 h under a positive nitrogen pressure. The resultant solution was evaporated, precipitated in an excess of ethyl ether and dried in vacuo. The dried polymer was dissolved in water and dialyzed for a week using Cellu SepH1 membrane with MWCO of 2000. The final product was obtained by lyophilization. PNIPAAm was synthesized and purified in the same way above, while PVL homopolymer obtained was precipitated in ethanol and collected by evaporation. In the same manner, the copolymers with different molar feed ratios were produced.

2.3. Gel permeation chromatography (GPC)

The molecular weights and molecular weight distributions of PNIPAAm-*co*-PVL and PNIPAAm were determined by gel permeation chromatography(GPC Waters 510/M32) using THF as a mobile phase with a flow rate of 1 ml/min. Monodisperse polystyrene (Polymer Laboratories Inc., MA) was used for calibration.

2.4. FTIR spectroscopy

FTIR spectra of copolymers and PNIPAAm were measured with the KBr disk using Bio-Rad FTS 135 spectrophotometer.

2.5. Elemental analysis

The contents of C, H, N in PNIPAAm homopolymer and copolymer samples were examined through ELEMENTAR vario EL.

2.6. LCST measurements

The LCSTs were determined by monitoring the optical density of the polymer aqueous solution at 500 nm as a function of temperature on a 756MC UV–vis spectrophotometer equipped with a thermostatic cell. The temperature was altered manually, and the solution was allowed to equilibrate for at least 15 min at each temperature. Pure water was used as a reference. The LCSTs were taken at the inflection point in the curves of optical density versus temperature.

2.7. Differential scanning calorimetry (DSC)

The thermal analysis of homo- and *co*-polymer solutions was performed on a Micro DSC III (SETARAM, France). 500–700 μl of sample solution was placed into a sealed sample cell. Heating scans were recorded in the range of 5–50 °C at a scan rate of 1 °C min^{-1}. Deionized water was used as a blank reference.

2.8. ^1H NMR spectroscopy

To estimate the composition ratios of copolymers, ^1H NMR spectra of PNIPAAm, PVL and copolymers were measured at ambient temperature with a Varian UNITY plus-400 NMR spectrometer using $CDCl_3$ as a solvent.

The LCSTs of PNIPAAm-*co*-PVL (in D_2O) were determined by in situ tracing the variation in the area of characteristic peaks on a programmed temperature-controllable Bruker AV-600 NMR spectrometer, where the copolymer samples with different concentrations were examined with interval temperature increase (control accuracy: ± 0.1 °C). For each sample, sufficient long time was kept at 7 °C and the signal area for NIPAAm segment ($-CH(CH_3)_2$, 3.59 ppm at 7 °C) was regarded as a standard, and the integration of other peaks or at other temperatures would be normalized relative to this standard. In order to have a reliable comparison among these characteristic signal data, the operative condition of spectrometer was kept the same for each measurement, and each temperature was kept for 30 min so that the deviation of integration of $-CH(CH_3)_2$ peak fell within ± 0.02.

2.9. Steady-state fluorescence spectroscopy

Steady-state fluorescence spectra were recorded on an SPEX FL212 Spectrofluorometer. For the determination of the intensity ratio of the first to the third highest energy bands (I_1/I_3) in the emission spectra of pyrene, the sample solutions containing pyrene (6.3×10^{-7} mol/l) were prepared and excited at 335 nm. The emission was measured between 350 and 600 nm at a scan rate of 10 nm/min. The slit openings for excitation and emission were set at 2.0 and 0.5 nm, respectively.

For measurement of fluorescence intensity at different temperatures, the sample was allowed to equilibrate for 30 min at each given temperature. The heating rate was controlled at 0.2 °C/min.

2.10. Dynamic light scattering

DLS measurements were performed on a laser scattering spectrometer (BI-200SM) with digital correlator (BI-9000AT) at 514 nm. Scattering angle was fixed at 90° and solution equilibrium was confirmed by the stability of scattering intensity at each temperature (± 0.1 °C) after equilibrium for 30 min. Levenberg-Marquardt method in nonlinear fitting program was used to fit parameters in the equations shown in the following section to analyze the time autocorrelation function-$g^{(2)}(\tau)$. CONTIN, the Laplace inversion program, was used to fit $g^{(1)}(\tau)$ in order to obtain information on micelle or cluster size distribution. The sample solutions were all filtered by 0.45 μm filter (Millipore) at room or lower temperature for dust removing.

3. Results and discussion

3.1. Characterization of PNIPAAm-co-PVL

In the FTIR spectra of PNIPAAm and copolymers with varied feed ratios, the absorbance bands at 1647 and 1538 cm^{-1} are assigned to secondary amide C=O stretching and secondary amide N–H stretching of PNIPAAm, respectively; while the sharp peaks at 1385, 1365 cm^{-1} correspond to the characteristic absorbance of isopropyl in PNIPAAm [18–20]. In comparison, the feature peak of VL around 1730 cm^{-1} (s, C=O, ester) is intensified with the increase of VL ratio in copolymers. In ^1H NMR spectra, the typical signals of PNIPAAm locate at δ 1.144, 1.671, 2.166 and 3.955 ppm [21–23]. For PVL, the characteristic peaks appear at δ 0.875 ppm. Furthermore, its bands at δ 0.875 ppm are also observed in copolymers, further confirming the occurrence of copolymerization.

The composition ratios (NIPAAm/VL, mol/mol) of the copolymers were estimated from the peak areas of $-CH(CH_3)_2$ (δ 3.955 ppm) and $-(CH_2)_{10}CH_3$ (δ 0.875 ppm) (Table 1). The molecular weight and distribution determined by GPC are listed in Table 1. Although the filtration problems might make the GPC results meaningless before samples enter the GPC column [24], and the irreversible chain aggregation may happen without residual trace amounts of water when drying a polymer sample [25], we adopted the method on GPC sample preparation proposed by Ganachaud [25]. It was reported that the molecular weight distributions characterized by GPC in THF with polystyrene standard were in good agreement with other methods in low molecular weight range ($\bar{M}_n \leq 5\times10^4$), and our GPC results show that $\bar{M}_n$ is in the range of $4–5\times10^3$; thus it is reasonable to consider that we have acquired reasonable molecular weight distribution data for homopolymer and copolymers. From Table 1, one can see that there is no significant difference in molecular weight distribution among these samples. It is necessary to point it out that we might obtain the same elution volume, that is, the same molecular weight from copolymers actually having different molecular weight due to the influence of monomer ratios on the hydrodynamic volume. Therefore, the molecular weight values shown in Table 1 are merely meaningful in their magnitude. Nonetheless, that is enough for our study, because in this experiment we only focused on the thermosensitive behavior of low molecular weight HM-PNIPAAm solution.

It is noted that PNIPAAm and PNI9.68VL1 were selected for purity analysis. The measured contents for PNIPAAm are 63.47%(C), 9.70%(H), 12.21%(N) (theory values: 63.71%(C), 9.73%(H), 12.39%(N)), and those for PNI9.68VL1 are 62.98%(C), 9.90%(H), 10.88%(N) (theory values: 62.88%(C), 9.93%(H), 10.92%(N)). Obviously, the measured contents of C, H and N in PNIPAAm and PNI9.68VL1 are in good accordance with the calculated ones, indicating high purity of the final products.

Table 1
The composition ratios, molecular weight distribution and CAC values of samples

Sample	Molar feed ratio NIPAAm/VL	Molar composition ratio NIPAAm/VL	$\bar{M}_n$	$\bar{M}_w$	$\bar{M}_w/\bar{M}_n$	CAC (mg/ml)
PNI9.68VL1	2:1	9.68:1	4357	6566	1.50	2.8×10^{-3}
PNI50VL1	16:1	50:1	4859	7049	1.45	4.1×10^{-2}
PNIPAAm			4441	7359	1.65	1.4

3.2. Turbidity and calorimetry study

3.2.1. Turbidity

Fig. 1 demonstrates the variation in turbidity of PNIPAAm and copolymer solutions as a function of temperature. It is evident that the turning points of optical density are LCSTs, which are dependent upon the solution concentration and hydrophobic moieties. The LCST of PNIPAAm solution at 52.0 mg/ml is located around 32 °C, whereas the LCST at 10.4 mg/ml shifts toward higher temperature, ca. 1 °C. In these two cases, PNIPAAm solutions show a sharp transition within merely 1 °C. In contrast, a lower LCST close to 20 °C is observed for PNI9.68VL1 solution at 52.0 mg/ml, and a similar variation trend of LCST is observed when the concentration of PNI9.68VL1 is diluted to 10.4 mg/ml. Its LCST, however, is shifted upward by 2.5 °C. Moreover, the transition range of PNI9.68VL1 at both concentrations is much broader relative to that of PNIPAAm, spanning at least 10 °C with solution changing from clear to totally milky state.

3.2.2. Micro-DSC

DSC has been widely used in the studies of PNIPAAm solution transition [18,26–28]. However, for PNI9.68VL1 solution, common DSC measurement cannot provide calorimetry data with acceptable signal noise ratio. Herein, we employed Micro-DSC to track the subtle transition with high sensitivity. Fig. 2 displays four endothermic peaks for PNIPAAm and PNI9.68VL samples. We can see that incorporation of hydrophobic segment and solution concentration influence the transition peaks. PNI9.68VL1 exhibits a broader transition locating at low temperature range compared with PNIPAAm. A possible explanation for the broader transition range of PNI9.68VL solution is that in our case, the copolymers were prepared with radical random copolymerization method, so the composition ratios in each copolymer chain cannot be well controlled, which results in a wide distribution of composition ratios in copolymers. Under this circumstance, the aqueous solution of copolymer displays a broader transition region.

The onset values of PNI9.86VL1 and PNIPAAm at 52.0 mg/ml representing the beginning transition temperatures, are located at 21.0 and 33.2 °C, respectively. The onset values of PNI9.86VL1 and PNIPAAm at 52.0 mg/ml correspond well with those LCST values tested through optical density method.

Table 2 demonstrates that the onset temperatures for both of PNI9.68VL1 and PNIPAAm solutions slightly decrease when the concentration is raised (also shown in Section 3.2.1). A reasonable explanation is that at higher concentration, the macromolecular chains entangle and overlap with each other, shortening the distance between

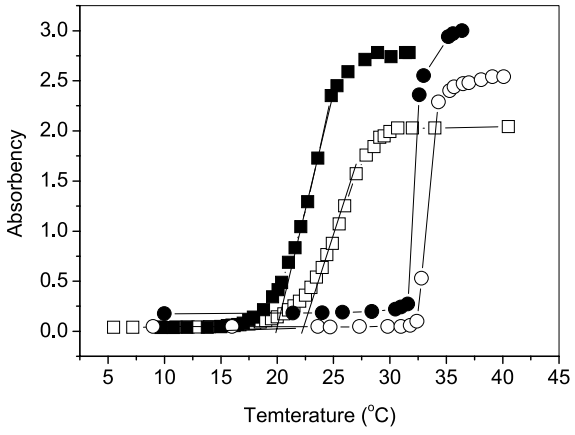

Fig. 1. Plots of absorbency at 500 nm as a function of solution temperature for PNIPAAm 10.4 mg/ml (○), PNIPAAm 52.0 mg/ml (●), PNI9.68VL1 10.4 mg/ml (□), PNI9.68VL1 52.0 mg/ml (■).

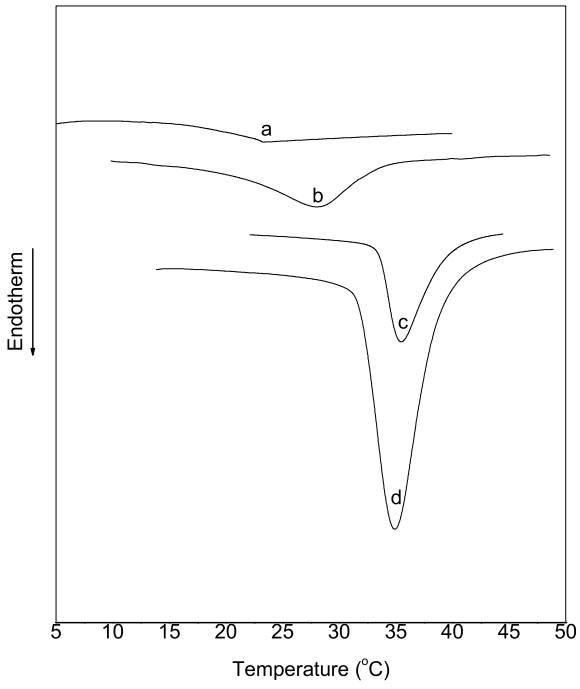

Fig. 2. Microcalorimetric endotherms for aqueous solutions of PNI9.68VL1 (52.0 mg/ml) (a), PNI9.68VL1 (231 mg/ml) (b), PNIPAAm (52.0 mg/ml) (c), and PNIPAAm (288.3 mg/ml) (d).

Table 2
Results of micro-DSC

Sample	Concentration (mg/ml)	Onset temperature (°C)	Peak temperature (°C)
PNI9.68VL1	52.0	21.0	23.3
PNI9.68VL1	231.0	19.2	28.2
PNIPAAm	52.0	33.2	35.2
PNIPAAm	288.3	31.6	35.0

hydrophobic moieties in polymer networks; hence, at lower temperature, the aggregation of hydrophobic groups is more inclined to occur. A similar behavior was also observed for PNIPAAm/poly(*N*-isopropylmethacrylamide) mixtures in D_2O [29].

From the table, it is seen that, however, the change trends of peak values are different between PNI9.86VL1 and PNIPAAm in that increasing concentration lowers the peak temperature of PNIPAAm but raises that of PNI9.68VL1. This may be attributed to the presence of hydrophobic moieties in PNI9.68VL1, delaying the completion of chain collapse.

3.3. Micropolarity study

3.3.1. Critical aggregation concentration (CAC)

Fig. 3 presents the change of I_1/I_3 as a function of polymer concentration for different samples. The critical aggregation concentration (CAC) is determined by the crossover of the two straight lines, which is the onset of self-association. The CAC values are summarized in Table 1. PNIPAAm shows the highest CAC (about 1.4 mg/ml) as expected; PNI50VL1 with one VL moiety per 50 PNIPAAm segments exhibits a lower CAC (4.1×10^{-2} mg/ml); For the most hydrophobic copolymer, PNI9.68VL1 with VL moieties accounting for 10% NIPAAm segments, its CAC is 2.8×10^{-3} mg/ml. Obviously, incorporating even 10% VL segments can lower CAC by 3 orders of magnitude, implying that a very strong hydrophobic interaction leads to the hydrophobic aggregation of macromolecular chains at extremely low concentration.

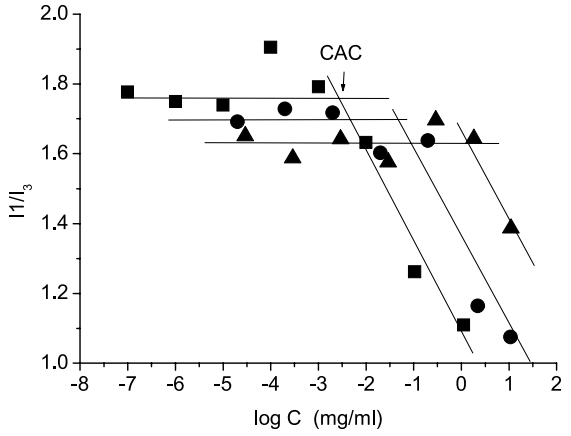

Fig. 3. Variation of I_1/I_3 vs. the concentrations of PNIPAAm (▲), PNI50VL1 (●) and PNI9.68VL1 (■) at room temperature (25 °C).

3.3.2. Temperature-induced polarity change

Fig. 4 demonstrates the micropolarity changes probed by pyrene at different temperatures for PNIPAAm and PNI9.68VL1 solutions at concentration of 0.1 mg/ml. The I_1/I_3 value of PNIPAAm remains nearly unchanged at temperature below 30 °C, above which it starts to decrease sharply. While for PNI9.68VL1, a broad increasing trend from about 20 to 35 °C is observed. Those trends are consistent with the previously reported work [11,12] that PNIPAAm and hydrophobically modified copolymers showed a totally different I_1/I_3 dependence upon temperature. As mentioned above, at 0.1 mg/ml, PNIPAAm displays no aggregation at temperature below its LCST, leaving most of pyrene probes locate in polar environment, which is reflected by a higher I_1/I_3 value (1.73). With temperature increase above the LCST, the collapsed PNIPAAm chains provide more of hydrophobic microdomains for pyrene solubilization, resulting in a polarity decrease with I_1/I_3 dropping to 1.51. In comparison, at the same concentration of PNI9.68VL1, an aggregation has occurred at room temperature, and the hydrophobic microdomains formed facilitate the solubilization of pyrene, generating a low value of I_1/I_3 at room temperature. Nevertheless, over temperature range from 20 to 35 °C, the microdomains undergo a mild rising process of polarity. Schild and Tirrell [11] attributed this 'abnormal' polarity change of highly hydrophobically-modified PNIPAAm to the penetration effect, that is, NIPAAm backbone units penetrate into the core formed by hydrophobic moieties, producing a more polar environment for pyrene probe. In the following section, we will demonstrate that the penetration is accompanied with a transition of isopropyl from hydration to dehydration as well as self-aggregation of hydrophobic chains at different temperature stages.

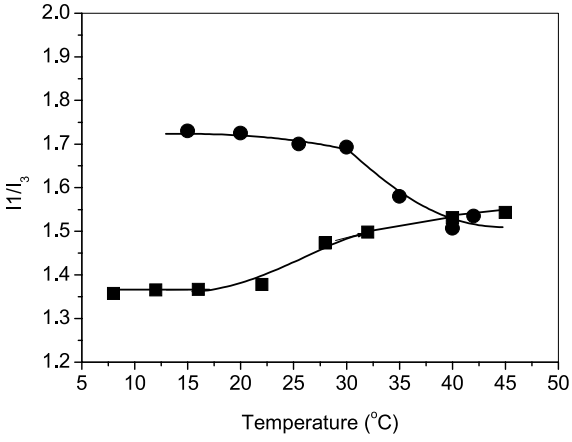

Fig. 4. Variation of I_1/I_3 vs. temperature for PNIPAAm (●) and PNI9.68VL1 (■) solutions. The concentration for both polymer samples is 0.1 mg/ml.

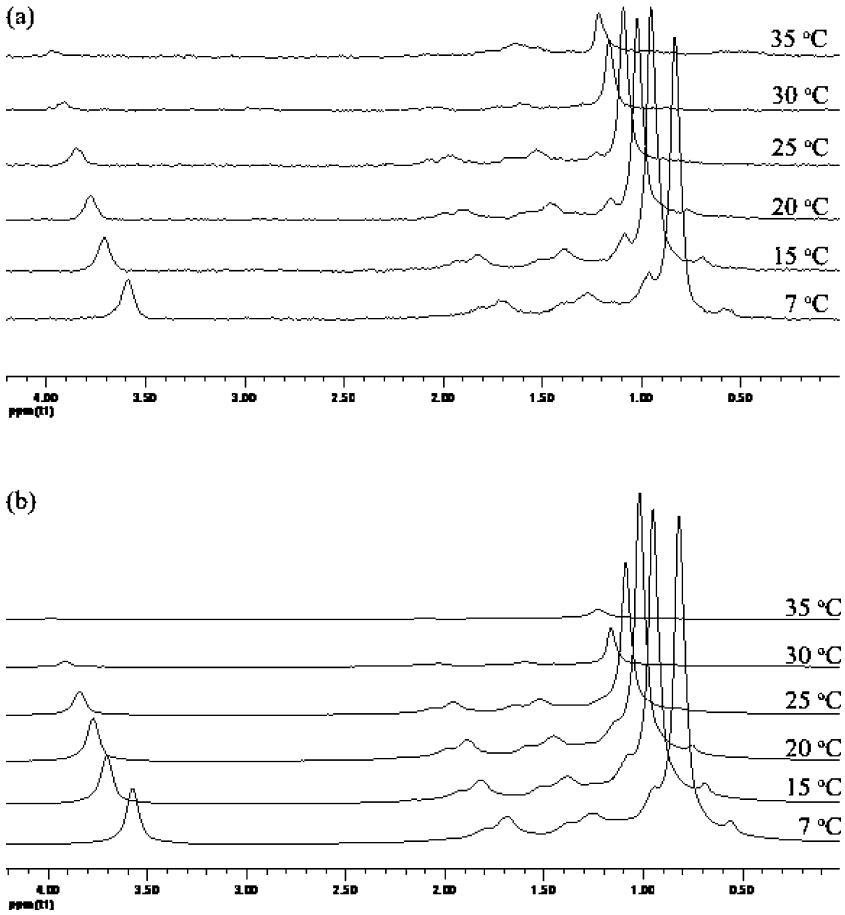

Fig. 5. ^{1}H NMR spectra at different temperatures for PNI9.68VL1 0.1 mg/ml (a) and PNI9.68VL1 52.0 mg/ml (b) in D_2O. In each group, all spectra (collected at the same condition) are zoomed in with the same degree as a guide to the eye.

3.4. *^{1}H NMR study of thermoresponsive transition behavior*

Since NMR can detect the thermoresponsive behavior at molecular level, we recorded the NMR spectra of PNI9.68VL1 and PNIPAAm at varied temperatures. Fig. 5 displays only the profiles of PNI9.68VL1, and those of PNIPAAm are not shown. We can see that the characteristic signals for VL ($-(CH_2)_{10}CH_3$, δ 0.56 ppm at 7 °C) at both concentrations are weakened along with temperature increase from 7 to 20 °C, and finally disappear at 25 °C. This indicates that the VL segments, at least methyl end groups, gradually enter or form the hydrophobic core of microdomains as temperature increases, and then turn to be totally undetectable in D_2O. As to NIPAAm segments in the PNI9.68VL1, they undergo a much broader hydration-dehydration phase transition in a much lower temperature range compared with the case of PNIPAAm homopolymer (Figs. 5 and 6).

Fig. 6 provides the detailed information on NIPAAm segments in PNI9.68VL1 and PNIPAAm, especially on the transition behavior of isopropyl groups, which can be characterized by the change of signal intensity (normalized). Apparently, the intensity of detectable isopropyl groups in PNI9.68VL1 at low concentration shows an almost continuous declining trend from 7 to 35 °C with a region of high decreasing rate from 20 to 30 °C. This trend becomes more significant for the sample at 52.0 mg/ml. The region (20–30 °C) detected is in good accordance with the optical density and fluorescence data shown in Figs. 1 and 4,

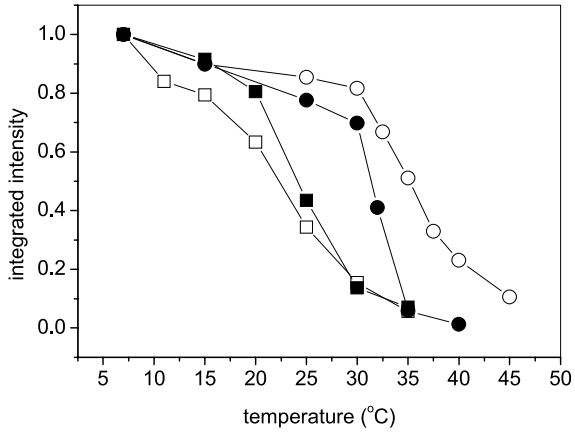

Fig. 6. Integrated proton intensity of isopropyl ($-CH(CH_3)_2$) normalized to ($-CH(CH_3)_2$) (3.59 ppm) at 7 °C as a function of temperature. PNIPAAm (0.1 mg/ml) (○), PNIPAAm (52.0 mg/ml) (●), PNI9.68VL1 (0.1 mg/ml) (□), PNI9.68VL1 (52.0 mg/ml) (■).

respectively, that is, from 20 to 30 °C isopropyl groups undergo the rapidest hydration–dehydration transition, and the solution property shows the greatest turbidity change and micropolarity change.

For PNI9.68VL1 sample, when temperature is as low as 7 °C (Fig. 6), the hydrophobic long alkyl side chains of PVL at high solution concentration (52 mg/ml) preferably self-aggregate, and generate more microdomains, which may entrap more of isopropyl groups or NIPAAm segments than those at low concentration (0.1 mg/ml), thus leaving less proportion of signal detectable in solution, that is, more of isopropyl moieties are entrapped in hydrophobic domains. Under these conditions, if we regard the area of isopropyl ($-CH(CH_3)_2$, 3.59 ppm at 7 °C) as 1, the intensity of isopropyl normalized to this standard at higher temperature will be lower than 1. From Fig. 6, the temperature-induced signal change in high concentration solution is less obvious than in low concentration in the range from 7 to 20 °C. This concentration effect may originate from the spatial barrier. While the temperature is below LCST (ca. 20 °C), the diffusion motion is dominant; thus for high concentration of PNI9.68VL1, isopropyl groups encounter more serious hindrance moving into hydrophobic domains, and consequently, causing more exposure of hydrated isopropyls; Above LCST (20–30 °C), the isopropyls in PNI9.68VL1 at 52 mg/ml show a relatively steeper declining trend, implying a possibility that at high concentration, the isopropyl groups facilitate the phase transition by providing profound chains entanglement.

Above 30 °C, the cases for PNIPAAm solution are almost the same as that of PNI9.68VL1 exceeding its LCST, i.e. a significant variation in signal intensity versus temperature at high concentration is observed. In regions below 15 °C, the curves of low and high concentrations are overlapped, indicating that the signal intensity is independent of concentration; from 15 to 30 °C, PNIPAAm backbones or isopropyl groups in high concentration solution have aggregated and formed hydrophobic domains, causing a relatively low signal detected. Obviously, the self-aggregation of isopropyls takes place prior to LCST, which is supposedly due to the fact that a broad molecular weight distribution exists in this system and the microphase separation is prone to happen even below LCST.

In our study, the variation in total proton intensity of the whole polymer chains as a function of temperature is also depicted in Fig. 7. Note that the total proton intensity is considered as 1 at 7 °C, and a similar normalization to the case of Fig. 6 is made. Here we expect to differentiate chain contribution between the local isopropyl groups and entire polymer chains during the phase transition. The curves of solid line and dot line are overlapped in the whole temperature range for PNIPAAm and PNI9.68VL1 at high concentration; the differences between the two become significant at low concentration. For PNIPAAm this difference happens above LCST; in contrast, the disparity occurs to PNI9.68VL1 almost over the whole temperature

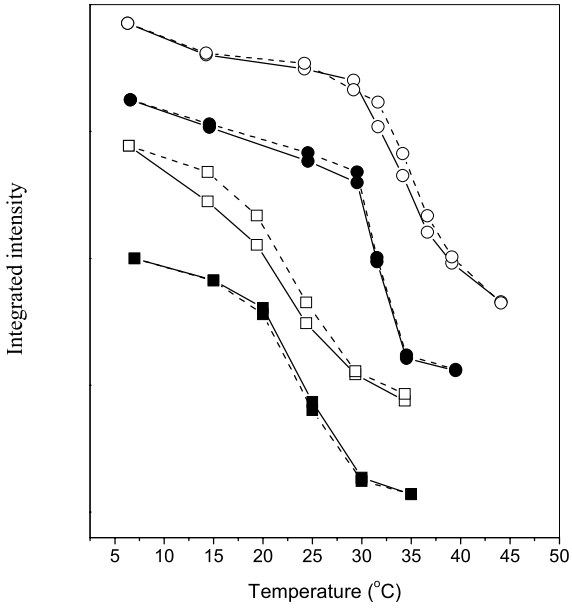

Fig. 7. Integrated proton intensity of isopropyl ($-CH(CH_3)_2$) normalized to ($-CH(CH_3)_2$) (3.59 ppm) at 7 °C as a function of temperature (solid line) and total proton intensity contributed by whole homopolymer or copolymer chains (dot line). PNIPAAm (0.1 mg/ml) (○), PNIPAAm (52.0 mg/ml) (●), PNI9.68VL1 (0.1 mg/ml) (□), PNI9.68VL1 (52.0 mg/ml) (■). The ordinate was translated as a guide to the eye.

range. It is apparent that for PNIPAAm at low concentration, isopropyl groups contribute more than the whole chains when temperature approaches LCST, showing a relatively sensitive signal variation or it is appropriate to say that more portions of isopropyl groups than the whole polymer chains participate in a hydration–dehydration transition. This discrepancy of contribution is resulted from more significant conformational transformations of isopropyl group than the backbones in phase transition process [21]. As to PNIPAAm at high concentration, this difference tends to disappear. It is surmised that a serious intra- or inter-molecular entanglement causes a more synergic phase transition for both isopropyl groups and entire chains. For PNI9.68VL1 at high concentration (52.0 mg/ml), a similar phenomenon is observed. However, PNI9.68VL1 (0.1 mg/ml) shows the greatest discrepancy among the four. A reasonable explanation for this is that below LCST, the VL segments have formed hydrophobic microdomains, which has a different accessibility for isopropyl groups and the entire chains during phase transition.

3.5. DLS

3.5.1. Intensity correlation function

PNI9.68VL1 samples were examined with DLS at different concentrations and different temperatures. Here we used normalized intensity correlation functions, $g^{(2)}(\tau)$ [30]. The following forms were used to analyze the normalized correlation data,

$$g^{(2)}(\tau) - 1 = \sigma_I^2\{A_f \exp(-\Gamma_f \tau)\}^2 \quad \text{(single exponential)} \tag{1}$$

$$g^{(2)}(\tau) - 1 = \sigma_I^2\{A_f \exp(-\Gamma_f \tau) + (1 - A_f)\exp(-\Gamma_{sl}\tau)^{\beta}\}^2 \quad \text{(single plus stretched exponential)} \tag{2}$$

where subscripts f, sl correspond to fast mode and slow mode, respectively. σ_I^2 is the initial amplitude, A the mode fraction, Γ the characteristic decay rate and β the stretched exponent ($0<\beta<1$).

Note that the single exponential, or the fast mode which is known to be the cooperative diffusion mode of chain segment between every two entangled points [31], does not fit well the correlation function $g^{(2)}(\tau)$, so we bring in the slow mode or the stretched part. In Eq. (2) fit, the slow mode is related to the translational diffusion mode of clusters.

Figs. 8 and 9 show the normalized intensity correlation functions of PNI9.68VL1 at high and low concentrations, respectively. Great changes of curve shape take place (relaxation time becomes faster) when temperature increases from 20 to 25 °C for both concentrations. In the temperature range from 25 to 40 °C, the curves in Fig. 8 overlap, while those in Fig. 9 exhibit different shapes. It should be pointed out that PNI9.68VL solution at 0.1 mg/ml remains clear over the whole selected temperature range. Therefore, the curve difference between 20 and 25 °C is caused by coil–globule transition, and other subtle differences among curves are the result of association in pre- and post-LCST region, which will be further confirmed by hydrodynamic diameter in later section. As to PNI9.68VL1 at 52.0 mg/ml, the solution has turned to milky state at 25 °C, and the turbidity is further enhanced as temperature

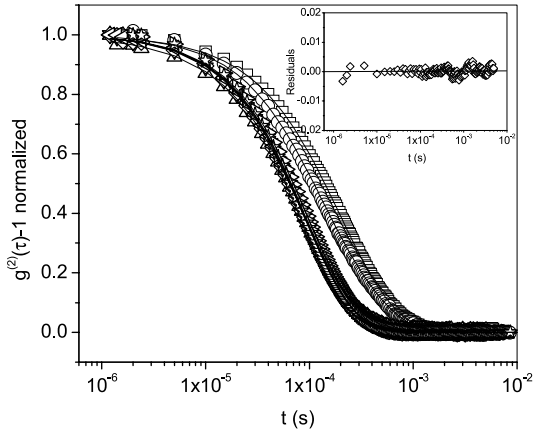

Fig. 8. Normalized intensity correlation functions of PNI9.68VL1 aqueous solution (0.1 mg/ml) at different temperatures. $\theta=90°$. (□) 15 °C, (○) 20 °C, (△) 25 °C, (▽) 27.5 °C, (◇) 30 °C, (◁) 32 °C, (▷) 35 °C, (☆) 40 °C. Solid curves are the results of single plus stretched exponential fits according to Eq. (5). The inset shows one example of residuals for curve fit at 30 °C.

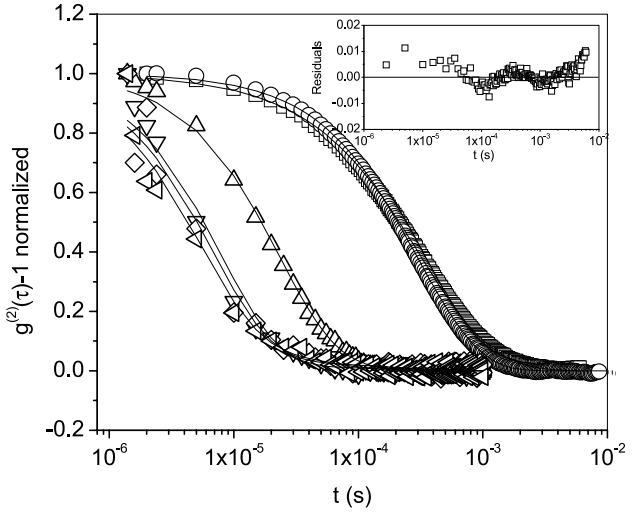

Fig. 9. Normalized intensity correlation functions of PNI9.68VL1 aqueous solution (52.0 mg/ml) at different temperatures. $\theta=90°$. (□) 15 °C, (○) 20 °C, (△) 25 °C, (▽) 30 °C, (◇) 35 °C, (◁) 40 °C. Solid curves are the results of single plus stretched exponential fits according to Eq. (5). The inset shows one example of residuals for curve fit at 15 °C. Curve fits for 30–35 °C are not successful as shown in this figure.

increases (shown in Fig. 1), resulting in different curve shapes in the range of 25–35 °C. This difference in the specific temperature range for high concentration solution reflects the weak scattering light due to the opacity of solution on the one hand, and on the other hand, suggests different particle sizes in milky solution though the hydrodynamic diameters calculated are within several nanometers, which is certainly incredible and will be discussed later.

Curve fits according to Eq. (2) are successful for PNI9.68VL1 at 0.1 mg/ml at all temperatures and 52.0 mg/ml at temperatures below 25 °C. Single plus stretched exponential fits are illustrated with small and nonsystematic residuals, e.g. the two inset plots in Figs. 8 and 9. Since single exponential fit is not suitable in our case at all, PNI9.68VL1 solution can be considered as sol state [32]. As to 52 mg/ml at temperatures above 25 °C, no proper curve fit is available in our work due to the scattered points collected for correlation functions.

3.5.2. Hydrodynamic diameter

Figs. 10 and 11 illustrate the hydrodynamic diameter distribution which was calculated through Stokes–Einstein equation (see Wu's work [33,34]) at different temperatures. For PNI9.68VL1 solution at 0.1 mg/ml, there exists a broad diameter distribution with average value being around 98.4 nm at 15 °C; while temperature is heated to 20 °C, the average size is increased to 102.2 nm due to self-aggregation of hydrophobic chains. The phase transition occurring at about 20–25 °C greatly lowers the hydrodynamic diameter and its distribution, reducing the diameter value by half compared to that at temperature below 20 °C, and the distribution becomes the smallest at 25 °C. With further

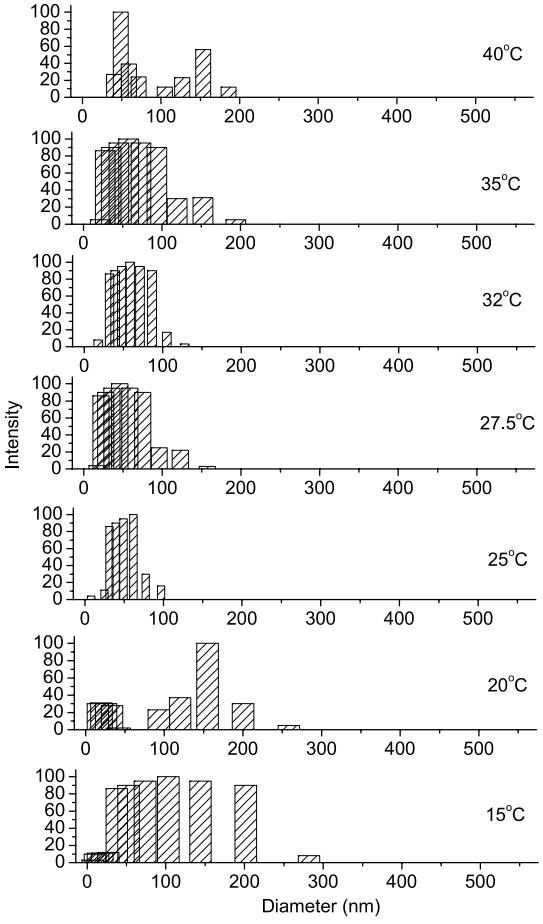

Fig. 10. Hydrodynamic diameter distribution of PNI9.68VL1 aqueous solution (0.1 mg/ml) at different temperatures analyzed with the CONTIN program ($\theta = 90°$).

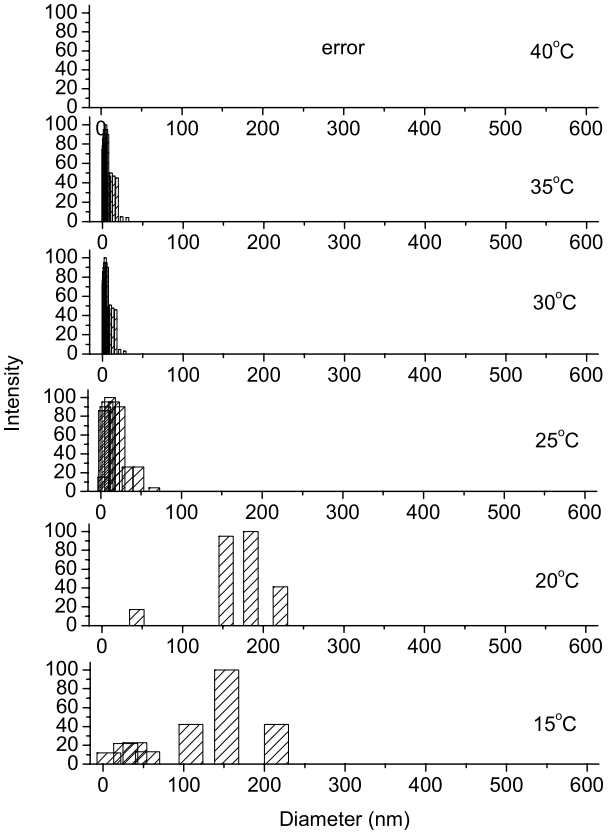

Fig. 11. Hydrodynamic diameter distribution of PNI9.68VL1 aqueous solution (52.0 mg/ml) at different temperatures analyzed with the CONTIN program ($\theta = 90°$).

heating, the macromolecular chains in solution undergo an aggregation, but the hydrophobic VL has induced the collapse of NIPAAm segments; hence merely a subtle increase of aggregate diameter and distribution appears.

For PNI9.68VL1 at 52 mg/ml, there appears a similar broad hydrodynamic distribution to 0.1 mg/ml solution below 20 °C, but the average size is increased up to 123 nm (15 °C) and 170 nm (20 °C), which is originated from larger aggregates formed at a high concentration. Also the diameter increase from 15 to 20 °C is much more evident relative to 0.1 mg/ml case, revealing that the pre-LCST aggregation is a significant temperature control process for high concentration samples. While 20–25 °C temperature range corresponds to phase transition process, the resulting hydrodynamic diameters estimated are less than 10 nm. Note that the hydrodynamic diameter in this case is generally equivalent to the correlation length or mesh sizes in gels. We argue that this solution at high temperatures forms gel-like aggregates with severely packing structure, though no macrogels form at this concentration. This mesh size becomes smaller and smaller along with heating above 25 °C, implying that a deep aggregation process has led to a more compact chain structure.

3.6. Conclusions

From the analysis above, the main conclusions are drawn as follows:

First, hydrophobic modification with PVL results in much lower and broader LCST regions of copolymer solutions. For PNIPAAm-*co*-VL solution with composition ratio of 9.68 (PNI9.68VL1), the LCST region spans 10 °C, and the hydrophobic microdomains have formed far below LCST, causing a significant aggregation process, which is controlled by both temperature and concentration. Moreover, the temperature has a more considerable effect on the aggregation behavior in the concentrated solution. Second, during the phase transition of PNI9.68VL1 solution, the penetration of PNIPAAm backbone into hydrophobic core is accompanied with a hydrated–dehydrated transition of isopropyl as well as a self-aggregation of hydrophobic chains. Third, while the entire chains of the copolymer participate in thermotransition, the local isopropyl groups contribute the most to the entry into hydrophobic microdomains at low concentration. However, the contribution of isopropyl groups is greatly weakened in the case of

concentrated solution where there exists a serious intra- or inter-molecular entanglement, which results in a more synergic phase transition for both isopropyl groups and entire chains.

The last, for PNI9.68VL1 solution at 0.1 mg/ml, the phase transition can be divided into three stages: pre-LCST aggregation (<20 °C), coil–globule transition at LCST(20–25 °C) and post-LCST aggregation(>25 °C). The hydrodynamic diameter shrinks abruptly from 20 to 25 °C, while optical density, micropolarity measurement and temperature-variable ^{1}H NMR show a continuous signal decrease from 20 to 30 °C (to our knowledge, it is the first work to trace segment solubility with temperature-adjustable NMR during phase transition). Although certain amount of isopropyl groups experience hydrated–dehydrated transition and micropolarity change above 25 °C, DLS gives no evidence of coil–globule transition with great shrink of hydrodynamic diameters. Thus, there might be a different mechanism between the penetration and coil–globule transition. The penetrating process is possibly a continuous hydrated–dehydrated transition over a wider temperature range, while a continuous coil–globule transition occurs in a relatively narrow temperature range.

Acknowledgements

The authors are indebted to the financial support from National Natural Science Foundation of China (Grant No. 30300086) and from the High Tech Research&Development (863) Program of China (Grant No. 2002AA326100).

References

[1] Hu T, You Y, Pan C, Wu C. J Phys Chem B 2002;106:6659.
[2] Balamurugan S, Mendez S, Balamurugan SS, O'Brien II MJ, Lopez GP. Langmuir 2003;19:2545.
[3] Kawasaki H, Sasaki S, Maeda H, Nishinari K. Langmuir 2000;16:3195.
[4] Schild HG. Prog Polym Sci 1992;17:163.
[5] Kurisawa M, Yokoyama M, Okano T. J Controlled Release 2000;69:127.
[6] Tsuda Y, Kikuchi A, Yamato M, Sakurai Y, Umezu M, Okano T. J Biomed Mater Res Part A 2004;69:70.
[7] Sun TL, Wang GJ, Feng L, Liu BQ, Ma YM, Jiang L, et al. Angew Chem, Int Ed 2004;43:357.
[8] Benaglia M, Puglisi A, Cozzi F. Chem Rev 2003;103:3401.
[9] Ibusuki S, Iwamoto Y, Matsuda T. Tissue Eng 2003;9:1133.
[10] Cho JH, Kim SH, Park KD, Jung MC, Yang WI, Han SW, et al. Biomaterials 2004;25:5743.
[11] Schild HG, Tirrell DA. Langmuir 1991;7:1319.
[12] Ringsdorf H, Venzmer J, Winnik FM. Macromolecules 1991;24:1678.
[13] Principi T, Goh CCE, Liu RCW, Winnik FM. Macromolecules 2000;33:2958.
[14] Spafford M, Polozova A, Winnik FM. Macromolecules 1998;31:7099.
[15] Nuopponen M, Ojala J, Tehu H. Polymer 2004;45:3643.
[16] Hay DNT, Rickert PG, Seifert S, Firestone MA. J Am Chem Soc 2004;126:2290.
[17] Benee LS, Snowden MJ, Chowdhry BZ. Langmuir 2002;18:6025.
[18] Shibayama M, Morimoto M, Nomura S. Macromolecules 1994;27:5060.
[19] Gupta KC, Khandekar K. Biomacromolecules 2003;4:758.
[20] Liu WG, Zhang BQ, Lu WW, Li XW, Zhu DW, Yao KD, et al. Biomaterials 2004;25:3005.
[21] Tokuhiro T, Amiya T, Mamada A, Tanaka T. Macromolecules 1991;24:2936.
[22] Zeng F, Tong Z, Feng HQ. Polymer 1997;38:5539.
[23] Deshmukh MV, Vaidya AA, Kulkarni MG, Rajamohanan PR, Ganapathy S. Polymer 2000;41:7951.
[24] Wu XY, Pelton RH, Tam KC, Woods DR, Hamielec AE. J Polym Sci, Part A: Polym Chem 1993;31:957.
[25] Ganachaud F, Monteiro MJ, Gilbert RG, Dourges MA, Thang SH, Rizzardo E. Macromolecules 2000;33:6738.
[26] Schild HG, Tirrell TA. J Phys Chem 1990;94:4352.
[27] Shibayama M, Mizutani S, Nomura S. Macromolecules 1996;29:2019.
[28] Otake K, Inomata H, Konno M, Saito S. Macromolecules 1990;23:283.
[29] Starovoytoval L, Spěváček J, Ilavský M. Polymer 2005;46:677.
[30] Chu B. Laser light scattering. 2nd ed. New York: Academic Press; 1991.
[31] de Gennes PG. Scaling concepts in polymer physics. Ithaca, NY: Cornell University Press; 1979.
[32] Shibayama M, Norisuye T. Bull Chem Soc Jpn 2002;75:641.
[33] Wu C, Zhou SQ. Macromolecules 1995;28:5388.
[34] Wu C, Zhou SQ. Macromolecules 1995;28:8381.